

Response surface study on production of explosively-welded aluminum-titanium laminates

E. S. EGE, O. T. INAL, C. A. ZIMMERLY

Materials and Metallurgical Engineering Department, New Mexico Tech, Socorro, NM 87801

This research was undertaken to produce strong and stiff, aluminum-titanium, multi-layered composites (laminates) by explosive welding, for applications requiring light-weight. The purpose of lamination is to create a material with superior mechanical properties resulting from plastic deformation produced by shock wave passage throughout each layer and from the presence of the explosively welded interfaces. A response surface study was performed on these laminates to investigate the mechanical behavior of the laminates with changes in two characteristic variables, abundance of interfaces and volume percentage of the more ductile component. For this purpose, a total of eighteen laminates, nine of which were the basis of a central composite design, were produced. One-step welding of these laminates was achieved by explosives-introduced pressuring; the material was supported by thicker steel plates on both sides to reduce the harmful effects of detonation and to produce smooth top and bottom surfaces. Yield strength, ultimate tensile strength, and elongation data were collected from tensile tests. A second-order model was fitted and a three dimensional response surface was built to define the relationship among the mechanical properties (yield strength) of the laminates and two design variables. The fitted second-order model clearly shows that the mechanical properties of the laminates depend strongly on the relative amounts of the components but only weakly on the abundance of interfaces within the selected operability region. © 1998 Kluwer Academic Publishers

1. Introduction

The main reason behind joining different metals (sheets) through explosive welding is to have uniform material flow and thus high strength and hardness throughout the material. In the case of laminates, several interfaces are assured since the interfaces are thought to be stronger than, at least, the weaker component. Strengthening in explosively-welded laminates is a combination of shock-induced hardening and the presence of well-adhered interfaces.

1.1. Multi-layered composites (laminates)

Typical multi-layered composites comprise of alternating layers of two or more different materials. Since laminates offer superior mechanical properties, especially strength-to-weight ratios, they have been an interesting subject of investigation for many researchers [1–6]. Metallic multi-layered composites have been produced by growth techniques such as sputtering [7], ionbeam deposition [8], and by brazing, roll bonding, and explosive welding [9–11].

Research on metallic, multi-layered composites produced by sputtering and electrodeposition is based on the idea of interfacial strengthening of the composite by placement of thin films in multilayers. For such structures, strength values based on hardness measurements are commonly used, since greater strengths are

expected perpendicular to the film planes. At greater film thicknesses, Hall-Petch strengthening is expected to be an important mechanism, since grain size perpendicular to the laminate plane diminishes with reduction of the laminate thicknesses. In the Hall-Petch model, the reason for the greater strength is smaller dislocation pile-ups formed near the laminate interfaces. These dislocation pile-ups force the leading dislocation to cross from one laminate to another. Decreasing the layer thickness reduces the number of dislocations possible in that pile-up; thus higher applied forces (stresses) would be needed. On the other hand, when the dislocation is constrained to a thin layer, an Orowan type of mechanism, in which the critical stress to propagate the dislocation is related to dislocation curvature, could be the dominant mechanism.

Also, Koehler proposed that the reason for greater strength was the differences in shear moduli and Burgers vector in each layer. Different shear moduli and Burgers vectors would mean a large difference in strain energy per unit length of dislocation (or line energy), $Gb^2/2$, which would be the real requirement for higher strengths. Koehler estimated a resolved shear stress, needed to drive dislocations across the interface, to be on the order of $G_{low}/100$, where G_{low} is the shear modulus of the less stiff component of the laminate.

Image forces are central to the strengthening in metallic laminates. Koehler theorized that there is an image

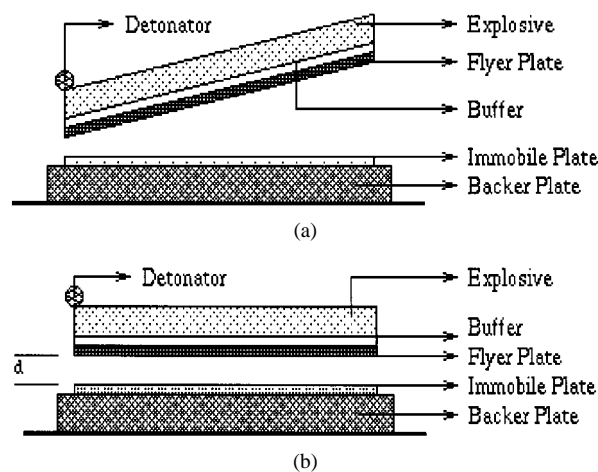


Figure 1 Typical two-plate assemblies for explosive welding: (a) inclined set-up and (b) parallel set-up.

stress that must be overcome to move a screw dislocation from a soft layer into hard layer against its own elastic image at the interface:

$$\tau_k^* = \frac{G_1(G_2 - G_1)b}{4\pi(G_1 + G_2)r} \quad (1)$$

where G_s are the shear moduli, b is the Burgers vector, and r is the distance of the related screw dislocation from the interface.

1.2. Explosive welding of sheets and laminates

In general, an explosive welding assembly for cladding flat sheets and plates contains a mobile and an immobile plate. In the case of lamination, although there is more than one mobile plate, the welding still can be achieved in a single step. The mobile plate in explosive welding is called the flyer plate. Flyer and parent plate (i.e., the immobile plate) can be welded explosively through either a parallel or an inclined set-up. Fig. 1 shows these two arrangements for two-plate assembly [12].

In the inclined set-up, it is possible to utilize the more efficient, more compact high-detonation-velocity explosives, with detonation velocities well above the sonic velocities of the metals being welded, because the maintained preset angle causes the process to proceed subsonically. In the parallel set-up, sub-sonic detonating explosives, with detonation velocities less than the sonic velocities of the metals being welded, are usually employed. This avoids component spalling and destruction.

The use of sub-sonic detonating explosives in the parallel set-up requires larger stand-off distances, since enough room is needed for acceleration. On the other hand, because the parameters can be varied over a wider range in the inclined set-up, the stand-off distance is generally smaller than the one used in the parallel set-up.

If the parent plate is thick enough, it might sit directly on the ground; otherwise it is placed on a thicker anvil. For thick parent plates, a bed of sand is an entirely satisfactory anvil; thinner parent plates require stronger anvils, such as a slab of steel or possibly concrete. The

stand-off distance, d , is maintained by wood, metal, or plastic inserts between the flyer and the parent plates at the very edges. To protect the surface of the parent plate from harmful effects of the explosive, a moderating layer (e.g. polyethylene, water, or rubber) is placed between the explosive and the prime metal. Above that buffer layer is the explosive charge which is stored in a plywood or cardboard box.

The necessary energy for explosive welding is provided by the detonation of an explosive. The explosives used in welding can vary both in detonation velocity and physical form. The physical forms of explosives utilized for welding include plastic flexible sheet, cord, pressed shapes, cast shapes, and powder or granulated explosives. Granulated explosives are very popular among operators, since they are easily transported and handled. In addition, most of the weldings are done with low to medium detonation velocity explosives, since they are capable of producing threshold detonation velocities for a large number of metal combinations. Other advantages of these kinds of explosives are that they require less buffering and are cheaper. They also allow for the use of a parallel arrangement that makes the process much simpler.

1.2.1. Explosive welding mechanism

Explosive welding, a solid-state technique, is achieved by application of pressure sufficient to cause large plastic deformation at the interface of the metallic components being welded. This plastic deformation increases the area of contact between the two components. The mobile plate in explosive welding is accelerated to very high velocities by the explosive-generated pressure. The collision with the immobile, parent plate, results in a rapid decrease in flyer plate velocity. This deceleration is converted into extreme pressures which make the two plates weld together. Since these high pressures break up the surface films at the collision point (jetting phenomenon), the clean metal surfaces are forced into intimate contact by the high pressure from the explosion. Although explosive welding is restricted to simple geometries, such as sheets, plates and tubes, it does not suffer from the same mechanical and metallurgical problems as fusion welding. These mechanical problems include heat-affected zones, differences in melting points of the metals, differences in thermal expansions, and an as-cast structure solidified under no pressure. The metallurgical problems of fusion welding can be summarized as formation of brittle intermetallics, alloy segregation, and reduced corrosion resistance; these are totally eliminated in explosive welding and, in contrast, a hardened layer formed from material flow renders the welded interface stronger than the weaker of the two metals joined.

1.2.2. Interface configuration

The metallurgical bond between two explosively welded metals might have two configurations, depending on the explosive welding parameters: straight, and wavy. Microscopic studies at and around the interfaces have revealed that heavy plastic flow occurs in these

regions. Earlier, the general belief was that the high strengths were not only because of the work-hardening around the interface, but also the mechanical interlocking effect of the interfacial waves. However, in wavy interfaces, molten pockets might be produced because of the adiabatic rise in temperature at each vortex of a wavy interface. This favors the formation of brittle intermetallics along the wavy interface. In straight (or planar) interfaces, there is no intermixing of species, thus there is no possibility of intermetallic formation along the straight interface.

1.3. Response surface methodology

Response surface methodology [13] is a union of statistical and mathematical techniques necessary for developing, improving, and optimizing processes. It is useful in the improvement of the existing product designs as well as designs of new products. RSM is used extensively in the industrial world to examine and characterize problems in which input variables influence some performance aspect of the product or process. This performance measure, or sometimes quality characteristic, is called the *response*. The input variables can also be called *independent variables* or *design variables*, since the designer or engineer is capable of altering them qualitatively and quantitatively. After the related model is fitted, a response surface might be built, since for each combination of independent variables there is a corresponding response variable. In addition to this three-dimensional graph, the response surface can also be demonstrated as a contour plot. This is a two-dimensional representation, and contour lines connect all the points that have the same value of response variable. The relationship between the response of a product, process, or system, y , and controllable input variables, $\xi_1, \xi_2, \xi_3, \dots, \xi_k$, can be written as:

$$y = f(\xi_1, \xi_2, \dots, \xi_k) + \varepsilon \quad (2)$$

where f is the true response function, and it is unknown and complicated, and ε is other sources of variability not accounted for within f (e.g. measurement error on the response, and intrinsic errors such as background noise, etc).

The variables $\xi_1, \xi_2, \dots, \xi_k$ in Equation 2 are called “natural variables”. They have the natural units of measurement. To facilitate the calculations, these natural variables are converted into “coded variables” x_1, x_2, \dots, x_k which are dimensionless parameters with zero mean and the same standard deviation. The conversion is accomplished by the following equation:

$$x_i = \frac{\xi_i - (\xi_{\text{low}} + \xi_{\text{high}})/2}{(\xi_{\text{high}} - \xi_{\text{low}})/2} \quad (3)$$

Since the form of the true response function is not exactly known, it must be approximated by a first-order or a second-order model. In general, the first-order model in terms of the coded variables is given as:

$$y = \beta_0 + \beta_1 x_1 + \beta_2 x_2 + \dots + \beta_k x_k + \varepsilon \quad (4)$$

A first-order model is more often used when there is little curvature in the true response function, f . It is convenient to use this model to approximate the true response surface over a small region of the independent variable space. Because Equation 4 is composed of only main effects of the independent variables, generally the corresponding response surface is a flat plane lying above the independent variables space.

The addition of interaction terms into the first-order model will introduce curvature in the response function.

A second-order model will be necessary unless the first-order model is adequate to characterize fully the curvature in the true response surface. This second-order model is also appropriate for approximating the true response surface in a relatively small region; however, the curvature is usually more pronounced.

The second-order model can be expressed as:

$$y = \beta_0 + \sum_{j=1}^k \beta_j x_j + \sum_{j=1}^k \beta_{jj} x_j^2 + \sum_{i < j} \beta_{ij} x_i x_j + \varepsilon \quad (5)$$

The models can be expressed in matrix notation to facilitate calculations:

$$y = x\beta + \varepsilon \quad (6)$$

where

$$y = \begin{bmatrix} y_1 \\ y_2 \\ \vdots \\ y_n \end{bmatrix}, \quad x = \begin{bmatrix} 1 & x_{11} & x_{12} & \dots & x_{1k} \\ 1 & x_{21} & x_{22} & \dots & x_{2k} \\ \vdots & \vdots & \vdots & \dots & \vdots \\ 1 & x_{n1} & x_{n2} & \dots & x_{nk} \end{bmatrix}$$

$$\beta = \begin{bmatrix} \beta_0 \\ \beta_1 \\ \vdots \\ \beta_k \end{bmatrix} \quad \text{and} \quad \varepsilon = \begin{bmatrix} \varepsilon_1 \\ \varepsilon_2 \\ \vdots \\ \varepsilon_n \end{bmatrix}$$

Generally, y is an $(n \times 1)$ vector of the observations, x is an $(n \times p)$ matrix of the levels of the independent variables, β is a $(p \times 1)$ vector of the regression coefficients, and ε is an $(n \times 1)$ vector of random errors.

2. Experimental

The experimental procedure consisted of joining the Al-Ti laminates by explosive welding, characterizing them by microhardness testing and optical microscopy, pulling them in tension, and eventually fitting the second-order model with the data collected from tensile testing.

2.1. Explosive welding

The laminated composites produced for the response surface study were made up of alternating layers of aluminum (6061) and titanium (6-4). A total of 18 shots were made. In the first six shots, various aluminum and

titanium alloys were used to establish the feasibility of the process and to determine the explosive welding parameters such as stand-off distance and detonation velocity, amount of explosive, etc. These explosive welding parameters were kept constant in later experiments. As a part of the response surface study, nine different sets of laminates were fabricated as defined by the central composite design. In these shots aluminum and titanium sheets having a size of 15.5 by 15.25 centimeters were used. Since explosive welding does not necessitate extensive cleaning of the welded surfaces, the sheets were roughly ground and cleaned with alcohol before welding. Titanium sheets were used as bottom layers, because of their higher strengths, whenever the central composite design allowed us to do so. Thicker low-carbon steel plates (20.30 × 20.30 × 0.15 cm) were glued to the very top layers as flyer plates. Acceleration of this flyer plate leads to collision and intimate contact of the sheets underneath. This flyer plate was used to eliminate the hazards of being in contact with the explosives.

In all shots, the parallel set-up was preferred over the inclined set-up for explosive welding; (thus explosives with slower detonation velocity could be utilized). To be able to ignore the effects of a possible texture on mechanical properties of the laminates, all assemblies were detonated in the rolling direction of the component sheets. The whole assembly was placed on a thick steel backer plate as displayed in Fig. 2.

Stand-off distances between each sheet changed in a decreasing fashion from the very top sheet to the very bottom sheet, since the stored kinetic energy decreases in the opposite direction.

The explosive utilized in the experiments was chosen to be of low to medium detonation velocity, since ex-

cessive kinetic energy stored at the interfaces was not desirable. For this reason, ammonium nitrate-fuel oil mixture (ANFO) was the proper explosive, and was the choice for all experiments. A high-velocity explosive, namely detasheet, was employed as the detonator and shock-wave initiator.

2.2. Characterization

Laminates obtained from one of the preliminary shots and nine other set of samples, produced according to the central composite design, were characterized. For this purpose, optical microscopy, microhardness testing and tensile testing were performed.

2.2.1. Optical microscopy

After having been cut, mounted, ground, and polished, the laminate samples were etched by immersing in Keller's reagent (1.0 ml conc. HF, 1.5 ml conc. HCl, 2.5 ml conc. HNO₃, 95.0 ml H₂O).

2.2.2. Microhardness testing

Microhardness indentations were taken along each layer of the composites by applying 300 for 15 seconds. The test was carried out on a Leco M-400 Hardness Tester with a Vickers indenter.

In each layer, several indentations were taken in interfacial regions and mid regions to give an idea about the depth of flow, i.e. work hardening achieved during the explosive welding procedure. Also, for comparison, the test was performed on unshocked aluminum and titanium samples.

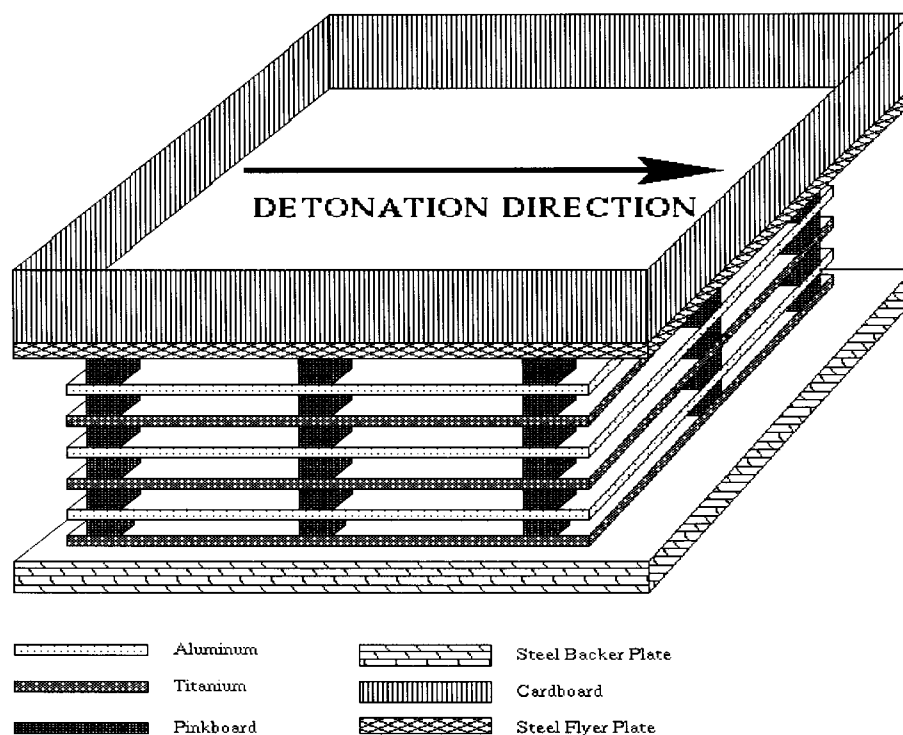


Figure 2 Experimental set-up for explosive welding of Al-Ti laminates.

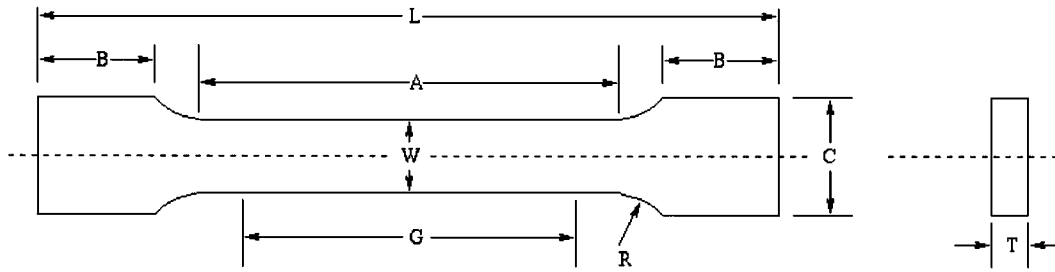


Figure 3 Typical sub-sized tensile test specimen where A = 15.90, B = 15.90, C = 4.80, L = 50.80, R = 3.20 and W = 3.20 (all in millimeters).

2.2.3. Tensile testing

Several specimens were prepared from each of the aluminum-titanium laminates, and unshocked aluminum and titanium components. A typical specimen is shown in Fig. 3. The samples were pulled in the rolling (detonation) direction. The test was performed with an MTS Servo-Hydraulic tensile testing machine. Testing was done at a strain rate of approximately $2 \times 10^{-4} \text{ s}^{-1}$. Yield strength, ultimate tensile strength, and percent elongation were calculated from the measurements.

2.3. Response surface study

The preliminary results showed that the mechanical properties of the laminates depended on the volume percentage and composition of the components. As suggested by the aforementioned theories, it was predicted that the abundance of interfaces (or total interfacial area) would affect the mechanical properties as well. The effects of changes in these variables on mechanical properties, such as yield strength, can be investigated by building an empirical model. This kind of model is based on observed or tested data from the experiments. In general, either a first-order model (e.g. linear regression model) or a second-order model (e.g. central composite design) is utilized according to the design requirements. A second-order model is superior in describing the curvatures of the established response surface. These kinds of models require sequential experimentation; in other words, a number of distinct design points must be chosen. To be able to fit a second-order response surface, at least three levels of each variable are required. Central composite design, where each variable has three levels, requires at least $1 + 2k + k(k - 1)/2$ distinct design points to build the corresponding second-order response surface. Here, k is the number of design variables. These design points are established by different combinations of three levels of the design variables.

In our design, the variables were chosen as volume percent of the more ductile metal and total interfacial area. Interfacial area could also be defined as density (abundance) of interfaces across the total thickness of the laminate, since a constant sheet size of 15.25 by 15.25 cm was used in all shots. Therefore, the first design variable, termed linear interfacial density, was taken as the number of interfaces divided by the total laminate thickness, and the second design variable was taken as volume percent of aluminum, which is the more ductile component of the multi-layered com-

TABLE I Three levels of aluminum content and interfacial density

	Low	Center	High
Volume fraction of the more ductile component (%)	38.50	49.25	60.00
Linear interfacial density (inch^{-1})	18.90	25.00	31.10

posite. In each laminate, the number of interfaces was one less than the total number of layers. Three levels of these two design variables are shown in Table I.

Once low and high levels of the volume percent of aluminum were defined, commercial availability of different Ti-6Al-4V sheet thicknesses was taken into account. In addition to that, for sheets of less than a certain thickness, explosive welding is quite difficult. This puts the following limitations on aluminum and titanium sheet thicknesses:

$$t_{\text{Al}} \geq 0.5 \text{ mm}$$

$$t_{\text{Ti}} \geq 0.4 \text{ mm}$$

where t_{Al} and t_{Ti} are thicknesses of aluminum and titanium sheets, respectively.

In central composite designs, the axial distance, α , usually changes between 1 and \sqrt{k} . The present central composite design, where axial distance was taken to be unity, is displayed in Fig. 4.

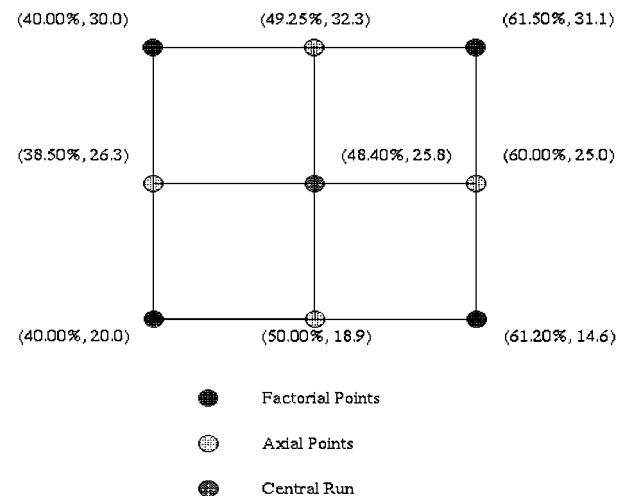


Figure 4 The central composite design for explosively-welded Al-Ti laminates.

TABLE II Experimental set-up for the central composite design

Shot No.	No. of Al layers	No. of Ti layers	Total number of layers	Al%	Interfacial density (inch ⁻¹)	t _{Al} (mm)	t _{Ti} (mm)
1	3	3	6	38.50	25.64	0.635	1.016
2	2	2	4	50.00	18.90	1.016	1.016
3	3	2	5	60.00	25.00	0.813	0.813
4	3	2	5	49.25	32.30	0.508	0.813
5	3	2	5	48.40	25.80	0.635	1.016
6	2	3	5	40.00	20.00	1.016	1.016
7	3	3	6	61.50	32.05	0.813	0.508
8	2	2	4	61.20	14.56	1.601	1.016
9	4	3	7	40.00	30.00	0.508	1.016

The model contained all the possible treatment combinations of 2² factorial design plus one central run, and four axial points. Table II describes the nine shots comprising the response surface study.

The method of least squares was employed to determine the unknown coefficients of the present model by the use of a statistical software, *Minitab* (1996) [14].

The design variables in Table II are expressed in the natural units of measurement (inch⁻¹, vol%). When the model was built, these natural variables were converted into coded variables by Equation 3 and the design matrix was determined as:

$X =$

I	x_1	x_2	x_1^2	x_2^2	x_1x_2
1	-1.004	0.105	1.008	0.011	-0.105
1	0.070	-1.000	0.005	1.000	-0.070
1	1.000	0.000	1.000	0.000	0.000
1	0.000	1.197	0.000	1.433	0.000
1	0.080	0.131	0.006	0.017	0.011
1	-0.860	-0.820	0.740	0.672	0.705
1	1.140	1.155	1.300	1.334	1.317
1	1.112	-0.951	1.237	0.904	-1.058
1	-0.860	0.820	0.740	0.672	-0.705

The first column in this matrix is the identity element and the unknown columns (third, fourth and fifth) were found by simply multiplying the values of the x_1 and x_2

components of the related columns. The response function matrix, y (9×1), was evaluated by tensile testing of component sheets and nine different laminates.

3. Results

All laminates along with one of the preliminary laminate were characterized by optical microscopy and microhardness testing. Before samples were tensile tested to collect data for the response surface study, it was assured that all interfaces were perfectly planar and a continuous material flow was achieved throughout the layers.

3.1. Preliminary laminate

This laminate is made of four layers of Ti-6-4 (.508 mm) and three layers of Al 6061 (.813 mm). Optical micrographs taken parallel and perpendicular to the welding direction show that the interfaces are perfectly planar in both directions (Fig. 5).

The mechanical properties of this set of laminates are summarized in Table III.

Hardening was observed especially in titanium layers (313.3 vs. 268.0 VHN). There was also hardening in aluminum layers to a lesser degree (121.1 vs. 108.6 VHN). Hardness values in the table are averages of hardness values taken from the interfacial and mid regions of the layers. Basically, hardness values of interfacial regions and mid regions of the layers exhibited no difference. This leads to the conclusion that hardening has occurred throughout each layer.

TABLE III Mechanical properties of the preliminary laminate

	Tested YS (MPa)	Tabulated YS ^a (MPa)	Tested SYS ^b (MPa*cc/g)	Tested UTS (MPa)	Tabulated UTS ^a (MPa)	Tested % elongation	Tabulated % elongation ^a	% in the laminate (by vol.)
Aluminum ^c	241.4	276.0	89.4	302.2	310.0	11.2	14.0	53.2
Titanium ^d	900.1	902.5	203.7	945.3	934.7	10.1	11.0	46.8
Laminate	632.4	NA ^e	180.2	715.8	NA ^e	6.8	NA ^e	100
ROM ^f	549.7	569.2	NA ^e	NA ^e	NA ^e	NA ^e	NA ^e	NA ^e

^a Metals Handbook [15,16].

^b Specific Yield Strength where $\rho(\text{Al}) = 2.7$, $\rho(\text{Ti-6-4}) = 4.43$, $\rho(\text{Lam}) = 3.51$ (all in g/cc).

^c 6061-T6 Aluminum.

^d Ti-6Al-4V (Annealed 835 °C, air cooled).

^e Not Applicable.

^f Rule-Of-Mixtures Expectation.

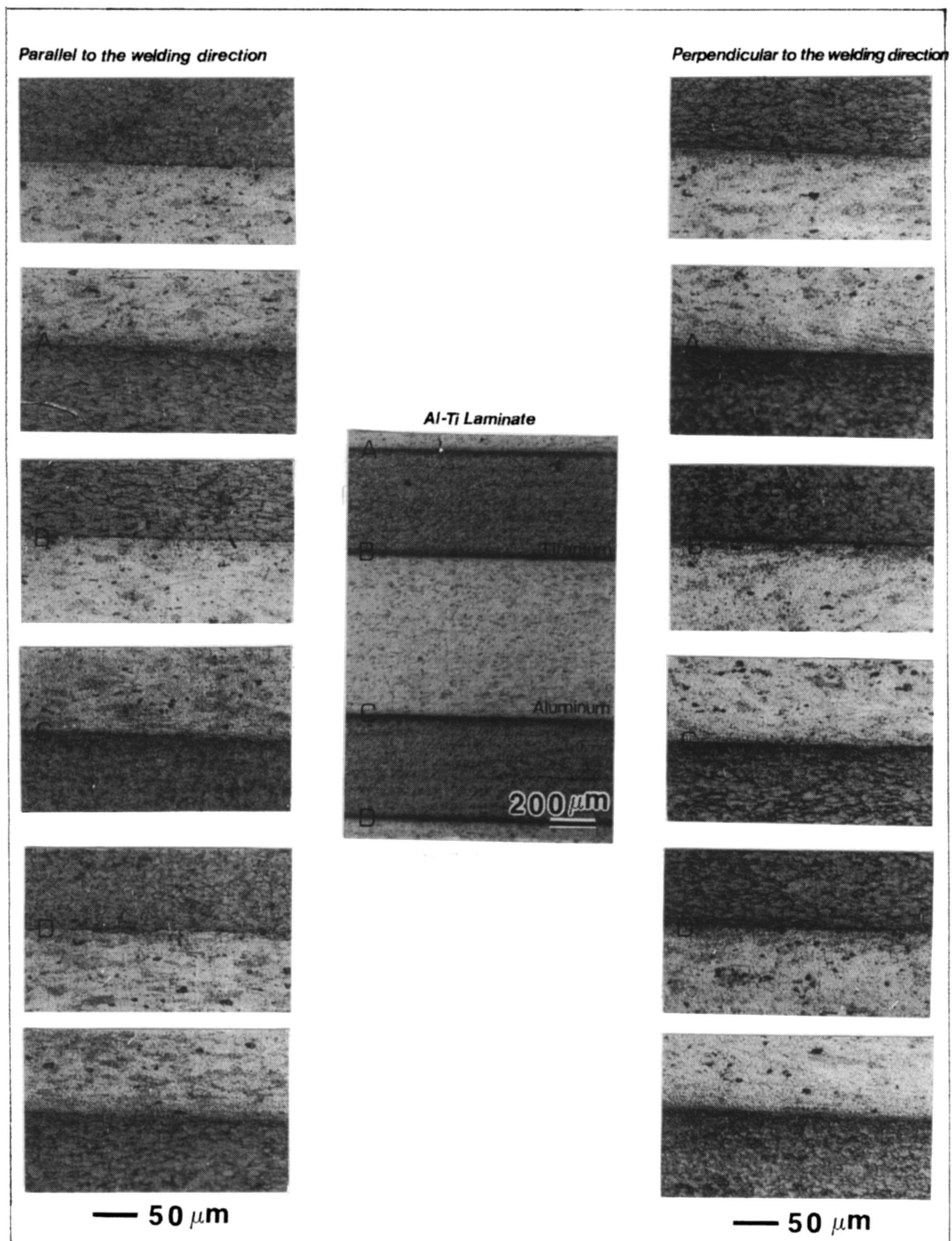


Figure 5 Preliminary laminate (Al 6061-T6/Ti-6Al-4V).

3.2. Tensile testing and model fitting

The yield strength data needed for a response surface study were collected from sequential tensile testing. The test results for the component sheets and the laminates are displayed in Tables IV and V, respectively.

Specific strengths in the tables were calculated by dividing the strength by density. The densities of aluminum (6061) and titanium (6-4) were taken as 2.7 g/cc and 4.43 g/cc, respectively. The densities of the laminates were calculated from rule-of-mixtures equation.

Since the aluminum and titanium sheets that made up the laminates exhibited mechanical properties that

depended on their thicknesses, yield strength values of the laminates were normalized with respect to one pair of aluminum and titanium sheets. The laminates # 1 and # 5 (Table II), which were made up of aluminum sheets having a thickness of 0.635 mm and titanium sheets having a thickness of 1.016 mm, were taken as the reference composites. For other laminates, two separate yield strength values were calculated from the rule-of-mixtures equation. The first one was calculated from the values listed in Table IV, the second was calculated from the strength values of the pair of reference sheets. The normalization procedure is summarized in Table VI.

TABLE IV Mechanical properties of the aluminum and titanium sheets

Sheet	Yield strength-(MPa)	Specific yield strength-(MPa*cc/g)	Ultimate tensile strength-(MPa)	Specific tensile strength-(MPa*cc/g)	% elongation
Al (0.508 mm)	256.9	95.1	294.4	109.0	11.9
Al (0.635 mm)	248.7	92.1	286.7	106.2	13.2
Al (0.813 mm)	241.4	89.4	283.0	104.8	11.2
Al (1.016 mm)	263.6	97.6	312.3	115.7	14.5
Al (1.601 mm)	255.5	94.6	298.7	110.6	14.8
Ti (0.508 mm)	900.1	203.2	945.3	213.4	10.1
Ti (0.813 mm)	845.4	190.8	908.1	205.0	10.9
Ti (1.016 mm)	874.4	197.4	925.8	209.0	10.7

TABLE V Mechanical properties of the laminates produced for response surface study

Lam. No.	Yield strength-(MPa)	Specific yield tensile strength ^a (MPa*cc/g)	Ultimate tensile strength-(MPa)	Specific strength-(MPa*cc/g)	% elongation
1	690.9	183.75	785.0	208.8	6.2
2	576.3	157.3	656.1	183.8	6.3
3	470.2	173.1	708.4	197.3	7.5
4	615.5	178.6	715.6	199.9	7.2
5	621.4	140.2	585.3	172.7	8.0
6	670.9	176.0	770.6	206.0	6.4
7	488.7	141.9	644.9	191.4	7.4
8	469.3	136.9	631.5	187.4	7.9
9	701.2	185.6	806.1	215.5	6.4

TABLE VI Normalization of the yield strengths

Lam. No.	Yield strength (MPa)	ROM _R (MPa)	ROM _A (MPa)	YS* ^($\frac{ROM_R}{ROM_A}$) (MPa)
1	690.9	633.8	633.8	690.9
2	576.3	561.6	569.0	568.8
3	470.2	499.0	496.3	472.8
4	615.5	566.3	555.6	627.4
5	621.4	571.6	571.6	571.6
6	670.9	624.1	630.1	664.5
7	488.7	489.6	495.0	483.4
8	469.3	491.5	495.7	465.3
9	701.2	624.1	627.4	697.7

The fitted second-order model in terms of coded variables is:

$$\hat{y} = 598.5 - 103.3x_1 + 18.8x_2 - 14.2x_1^2 + 4.7x_2^2 - 6.0x_1x_2 \quad (7)$$

where \hat{y} is the predicted yield strength, x_1 is the volume percentage of aluminum and x_2 is linear interfacial density.

This second-order model suggests that the yield strength of the laminates increases as the volume percentage of aluminum decreases and the interfacial density increases.

However, the larger coefficient of volume percentage of aluminum means that the yield strength more strongly depends on this variable than on interfacial density. This conclusion can also be verified by visual examination of the response surface and contour plots

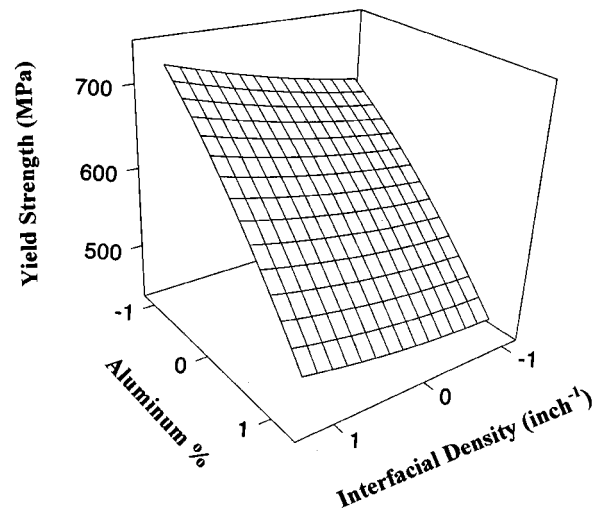


Figure 6 Response surface of the yield strength predicted by the second-order model.

of predicted yield strength (Figs 6 and 7). The way the response surface is inclined and the steep contour lines are in good agreement with this judgement.

The R^2 and adjusted R^2 (R^2_{adj}) values for this second-order model are 99.5% and 98.8%, respectively. The normality assumption is satisfied and the residuals scatter randomly according to the residual analysis performed for this second-order model (Fig. 8). Since these two assumptions are satisfied, there is no need for a transformation of the response function, y , into a curative measure. Usually the remedy involves transformation of the response into a logarithmic function.

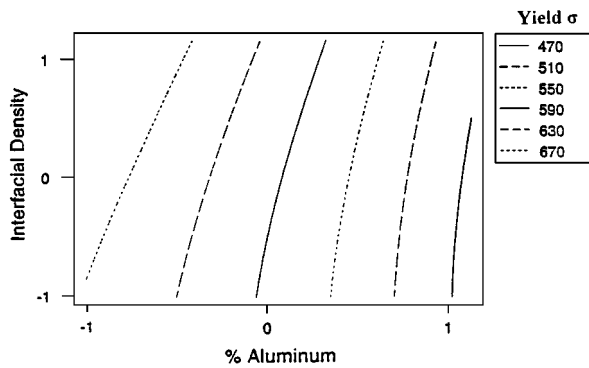


Figure 7 Contour plot of the yield strength predicted by the second-order model.

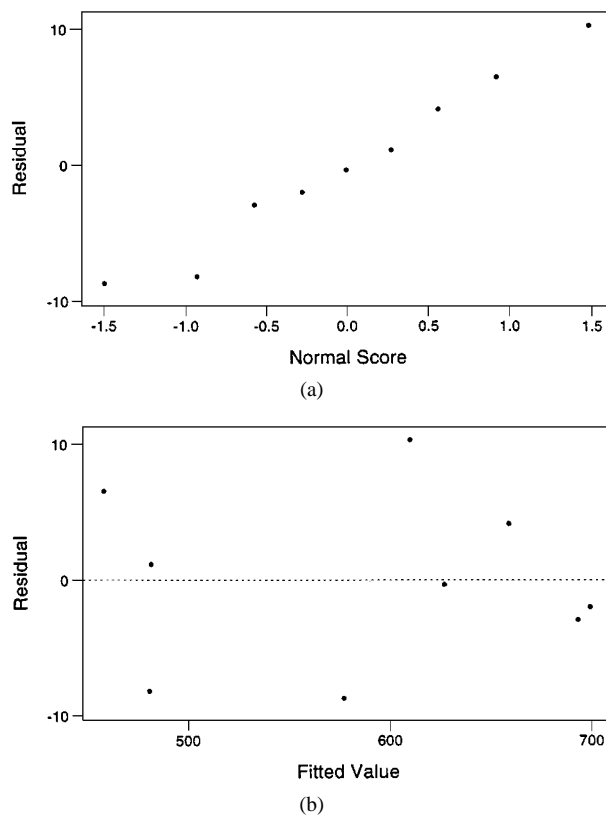


Figure 8 Residual analysis: (a) normal probability of the residuals and (b) residuals versus the fitted values.

4. Discussion

In the present study, explosive-welding was utilized to join aluminum and titanium sheets of thicknesses in the range 0.508 to 1.601 mm. Tensile strengths as high as 825 MPa were achieved, depending on the relative amounts of aluminum and titanium in the composite. Yield strengths of the laminates are higher than the ones calculated from rule-of-mixtures equation (although a few exceptions occurred in the case of laminates in which the top and the bottom layers are aluminum). At these relatively large thicknesses, the dominant strengthening mechanism was expected to be hardening produced by shock-wave passage. The fitted second-order model, which employs aluminum content and interfacial density as indicators of strengthening by shock-waves and by the Koehler mechanism,

respectively, is also in good agreement with this expectation. A coefficient of aluminum content much larger than the coefficient of interfacial density in Equation 7 indicates that the former variable is dominant and that shock-induced hardening is substantially more important than Koehler strengthening.

The results of the response surface study can be more efficiently interpreted if the yield strength values are plotted against one of the design variables at different constant values of that design variable. Fig. 9 shows the plots of yield strength versus aluminum content at low, medium and high levels of interfacial density. Since the effect of interfacial density on yield strength is small, the lines are very close, and almost coincident at low titanium contents. The explanation for this behavior could be that titanium work hardens more rapidly than aluminum. In Fig. 10, yield strength is plotted against interfacial density at three levels of aluminum content. This plot, once again, reveals the dominance the effect of aluminum content on the mechanical properties of laminates. Nevertheless, the beneficial effect of interfacial density is real.

The densities of the laminates only depend on the relative amounts of the components. The density of a particular laminate can be calculated from the following rule-of-mixtures equation:

$$\rho = \frac{2.7A1\%}{100} + 4.43 \left(\frac{100 - A1\%}{100} \right) \quad (8)$$

$$\rho = 4.43 - 0.0173A1\% \quad (8.1)$$

where ρ and A1% are the density and aluminum content of the laminate, respectively, and 2.7 and 4.43 g/cc are the densities of Al 6061 and Ti-6-4, respectively.

In Fig. 11, yield strength is plotted versus density, calculated from Equation 8.1, at three levels of interfacial density. As expected, the trend observed in the plot of yield strength versus aluminum content can also be seen in this plot. It is possible to achieve higher strengths by increasing the titanium content, which in turn increases the density of the laminate. However, employing the maximum interfacial density in the operability region lets one obtain the same high strength at a lower density.

As mentioned earlier, one of the aims behind producing these laminates is to achieve high strengths at lower densities. Upon investigation of Tables IV and V, it is seen that some titanium-rich laminates exhibit higher specific strength values than plain, annealed Ti-6-4. In Fig. 12, specific strength is plotted versus aluminum content at three levels of interfacial density. The trend follows almost the same curve for each level of interfacial density. At high titanium contents, it is possible to obtain higher specific strengths than Ti-6-4, although at a lower ductility. To be able to benefit fully from the presence of interfaces, the highest level of interfacial density should be assured in the operability region. Laminates with high specific strengths can be achieved at high densities. Since these specific strengths

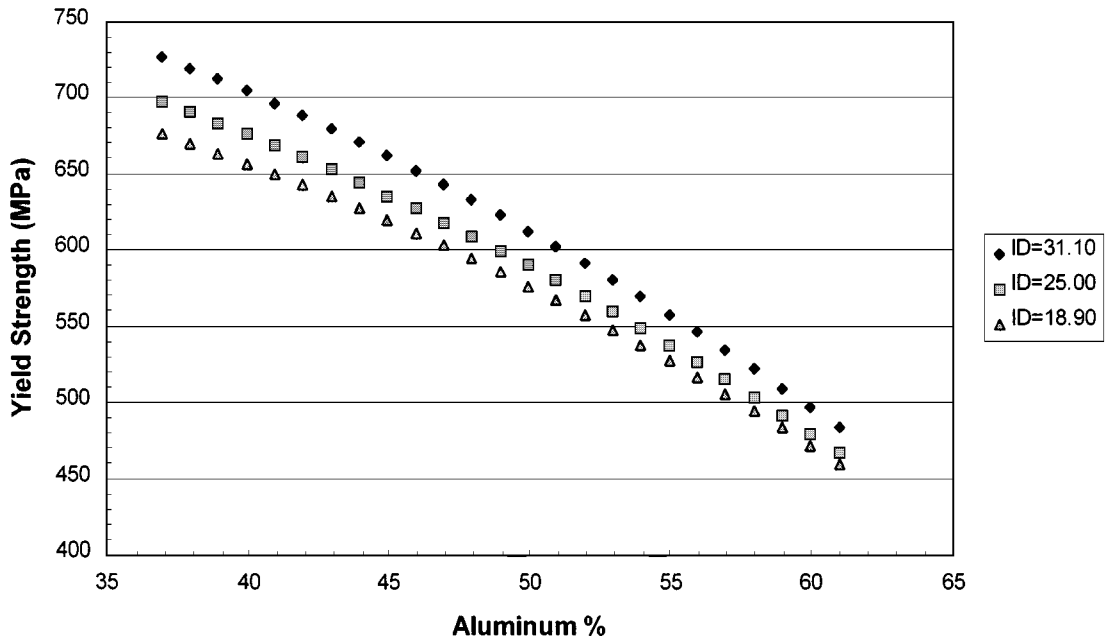


Figure 9 Yield strength versus aluminum content at three levels of interfacial density.

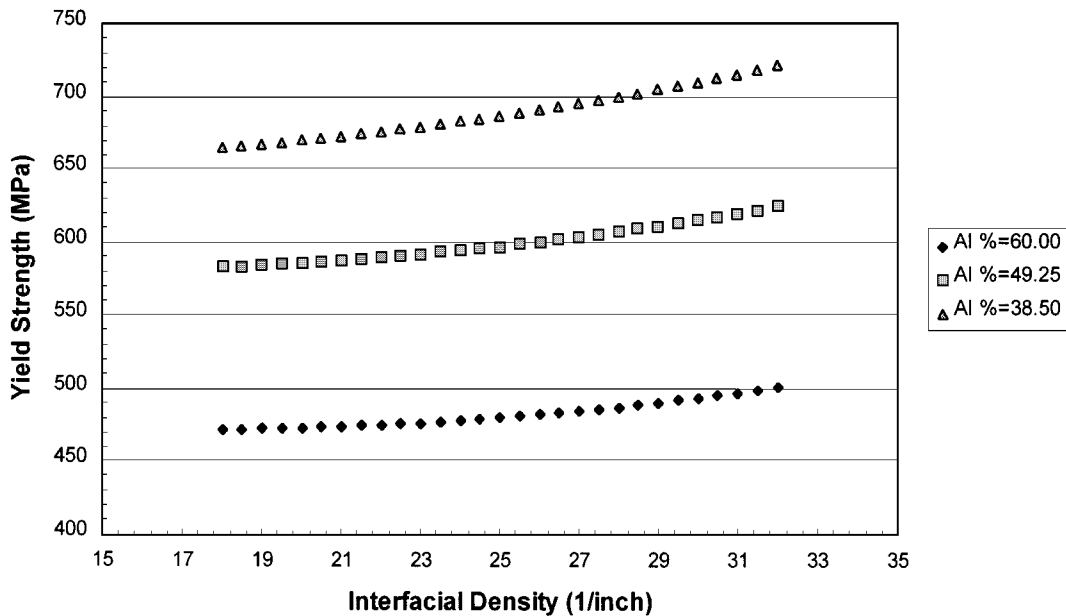


Figure 10 Yield strength versus interfacial density at three levels of aluminum content.

can compete with that of titanium, it may be possible to produce laminates that can sustain large loads at volumes close to that of titanium.

As seen in the contour plot of yield strength, the fitted model is composed of declining (or rising) contours. It does not possess any maximum, minimum or saddle point. This means that there is no single laminate combination of aluminum content and interfacial density that has the best mechanical properties. Nevertheless, the fitted second-order model is important for selecting the laminate that best fulfills specific strength and density requirements.

For example, a laminate is to be designed for a certain yield strength at minimum density. This laminate can be produced by different combinations of aluminum content and interfacial density in the operability region. Upon examination of Fig. 12, the laminate having the

highest yield strength with minimum density is the one with the highest level of interfacial density (31.10) in the operability region. Since the density of this laminate is determined, the corresponding aluminum content can be found by Equation 8.1. As two main design variables, aluminum content and interfacial density, are fixed, a number of different combinations of aluminum and titanium sheets can be utilized to produce a laminate of given thickness. However, the density benefit at a constant strength conferred by a high level of interfacial density versus a low level of interfacial density is not more than 4%. This means that the presence of interfaces is not as beneficial as was hoped. However, by further optimizing the explosive welding, the operability region might be widened and laminates with more abundant interfaces could be produced to further delineate this effect.

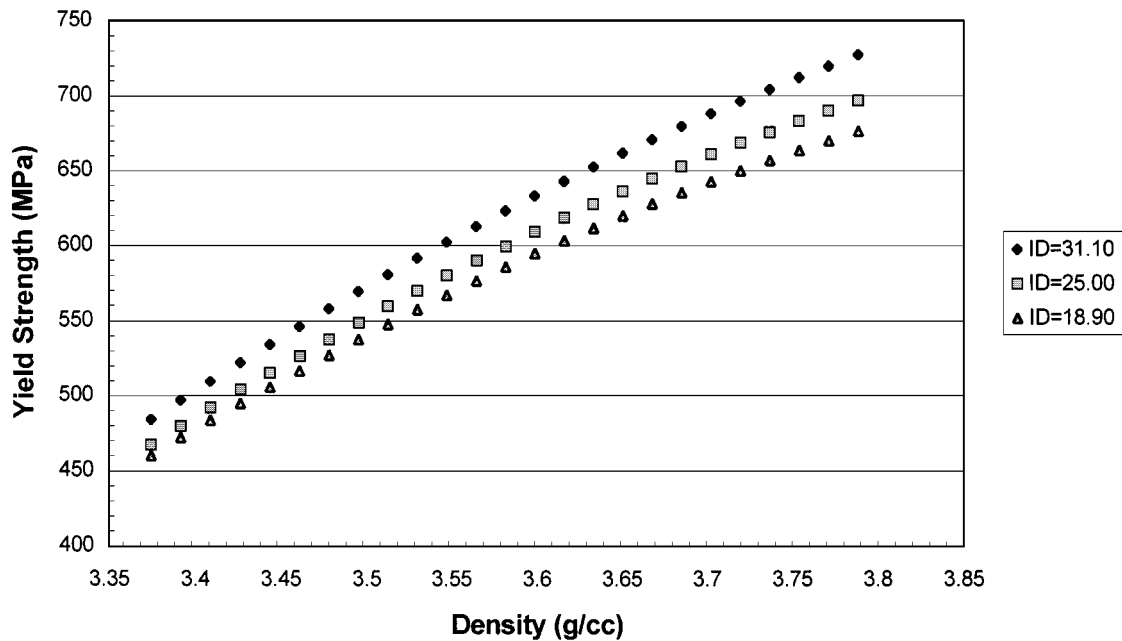


Figure 11 Yield strength versus density at three levels of interfacial density.

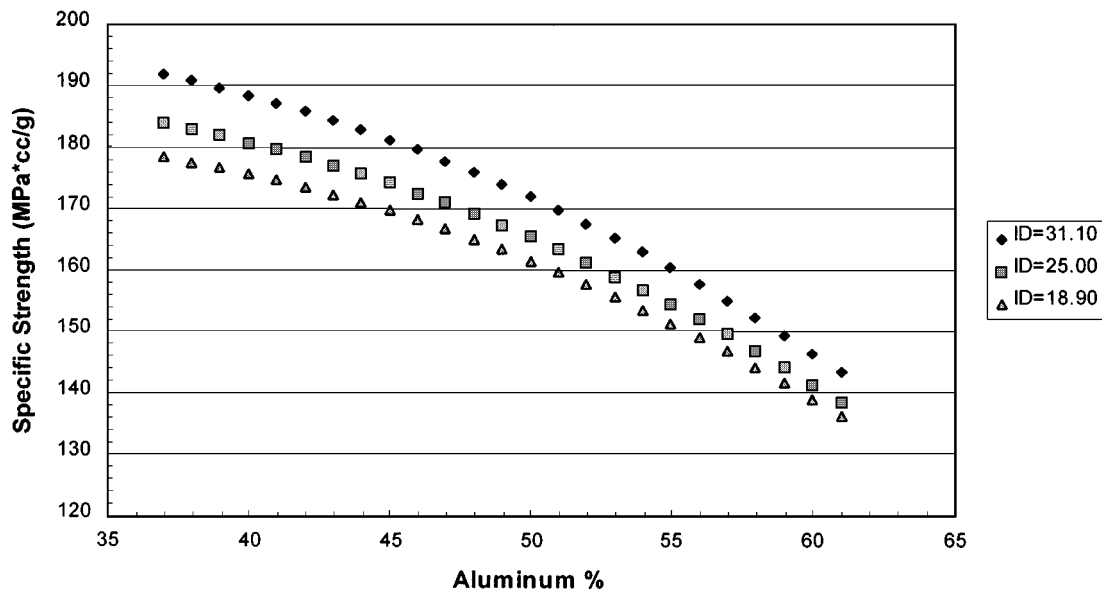


Figure 12 Specific strength versus aluminum content at three levels of interfacial density.

5. Conclusions

Aluminum-titanium multi layered composites (laminates), with uniform hardness throughout each layer, were successfully fabricated through explosive welding. Strength-to-weight ratios close to that of titanium were achieved.

The fitted second-order model, based on volume percentage of aluminum and linear interfacial density as design variables, showed that hardening produced by shock-wave passage contributed to strengthening much more than Koehler strengthening induced by elastic moduli mismatch.

With the fitted second-order model, along with a series of plots, it is possible to fabricate laminates that are tailored to strength, density and load specifications.

The dominance of strengthening produced by shock-wave passage could be a consequence of the narrow op-

erability region of the central composite design, and deficiencies associated with explosive welding performed without an initial, extensive parameter optimization.

References

1. D. TENCH and J. WHITE, *Metallurgical Trans.* **15A** (1984) 2039–2056.
2. S. L. LEHOCZKY, *J. Appl. Phys.* **49** (1978) 5479–5485.
3. U. HELMERSSON, S. TODOROVA, S. A. BARNETT and J-E. SUNDGREN, *ibid.* **62** (1987) 481–484.
4. C. A. HOFFMAN and J. W. WEETON, *Metallurgical Trans.* **5** (1974) 309–315.
5. D. BARAL, J. B. KETTERSON and J. E. HILLIARD, *J. Appl. Phys.* **57** (1985) 1076–1083.
6. B. S. BERRY and W. C. PRITCHET, *Thin Solid Films* **33** (1976) 19–28.
7. D. P. ADAMS, M. VILL, J. TAO, J. C. BILLELO and S. M. YALISOVE, *J. Appl. Phys.* **74**(2) (1993) 1015–1021.

8. C. SARRAZIN, J. P. RIVIÈRE and R. J. GABORIAUD, *Physica Status Solidi, Applied Research*, **A 107** (1988) 867–871.
9. S. A. L. SALEM and S. T. S. AL-HASSANI, in “Shock Waves and High Strain Rate Phenomena in Metals,” edited by M. A. Meyers and L. E. Murr (Plenum Press, New York) pp. 1003–1018.
10. S. N. SHOUKRY and A. A. HEGAZY, *Propellants, Explosives, Pyrotechnics* **13** (1988) 144–148.
11. K. HOKAMOTO, A. CHIBA and M. FUJITA, *Compos. Eng.* **5**(8) (1995) 1069–1079.
12. M. M. SCHWARTZ, “Metals Joining Manual” (McGraw-Hill Book Company, USA, 1979) Section 5.
13. R. H. MYERS and D. C. MONTGOMERY, “Response Surface Methodology,” (John Wiley & Sons, USA, 1995).
14. B. F. RYAN and B. L. JOINER, “Minitab Handbook” (Duxbury Press, Belmont, CA, 1994).
15. “Metals Handbook,” Vol. 2, (ASM International, USA, 1990) p. 62.
16. “Metals Handbook,” Vol. 2, (ASM International, USA, 1990) p. 592.

*Received 11 September
and accepted 14 September 1998*